IEEE Photonics Journal
An IEEE Photonics Society Publication

Open Access

Study on Growth Process of Ag(In, Ga)Se_2 Films by a Three-Stage Co-Evaporation Method Using Molecular Beam Epitaxy Apparatus

Volume 9, Number 2, April 2017

Xianfeng Zhang
Masakazu Kobayashi

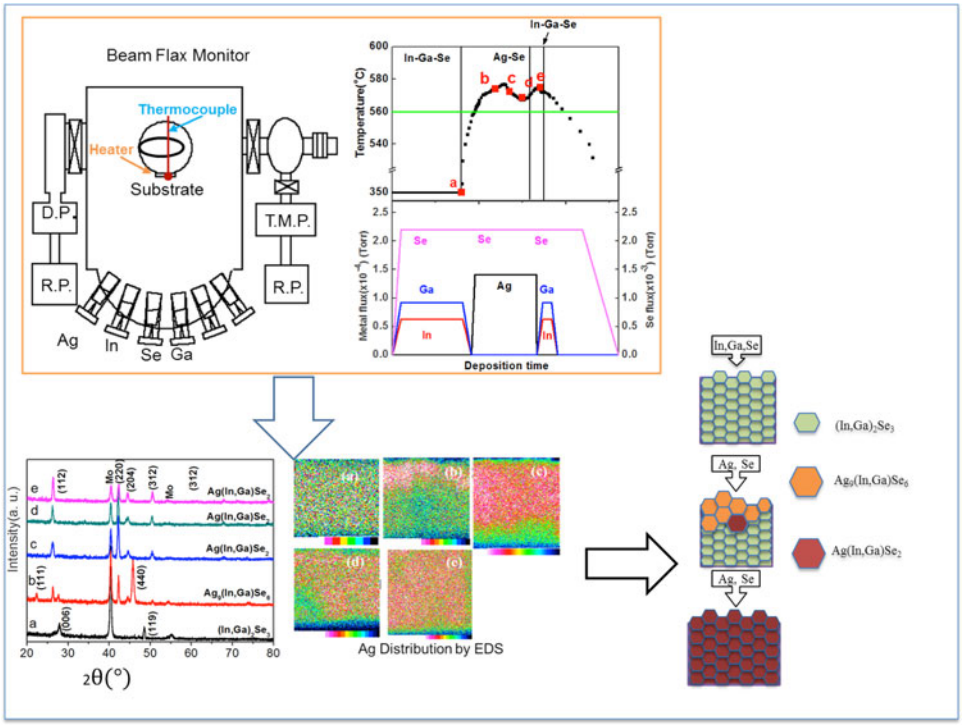

DOI: 10.1109/JPHOT.2017.2670923
1943-0655 © 2017 IEEE

Study on Growth Process of Ag(In, Ga)Se_2 Films by a Three-Stage Co-Evaporation Method Using Molecular Beam Epitaxy Apparatus

Xianfeng Zhang[1] and Masakazu Kobayashi[2]

[1]International Center for Science and Engineering Programs, Waseda University, Tokyo 169-8555, Japan
[2]Department of Electrical Engineering and Bioscience and Kagami Memorial Research Institute for Materials Science, Waseda University, Tokyo 169-8555, Japan

DOI:10.1109/JPHOT.2017.2670923

Manuscript received February 2, 2017; revised February 13, 2017; accepted February 14, 2017. Date of publication February 17, 2017; date of current version March 10, 2017. This work was supported by the New Energy and Industrial Technology Development Organization, Japan. Corresponding author: X. Zhang (e-mail: zhangxf@aoni.waseda.jp).

Abstract: Ag(In, Ga)Se_2 (AIGS) has been considered as a promising candidate material for the top cell of chalcopyrite-based tandem solar cells. In this work, the process of (AIGS) film growth by a three-stage molecular beam epitaxy method is studied. The diffusion of silver and grain growth of AIGS films from the first stage-deposited (In, Ga)$_2Se_3$ is investigated. Energy dispersive spectroscopy mapping is used to reveal the distribution of silver in the film during each stage of the deposition process. A sharp silver accumulation at the surface of the film at the early stage of the deposition process is observed. This has led to the formation of a silver-rich phase, which gradually diffused into the film to produce a homogeneous distribution. X-ray diffraction results illustrate the phase changes of AIGS films. Based on the result, a growth model for AIGS films from the first stage to the second stage is suggested as (In, Ga)$_2Se_3$ $\rightarrow$ Ag_9 (In, Ga)Se_6 at the surface and (In, Ga)$_2Se_3$ at the bottom of the film $\rightarrow$ silver-rich AIGS film. During the third stage, the silver-rich film was converted to silver-poor film. The performance of AIGS solar cells fabricated from various samples was compared, and a highest efficiency of 7.1% was obtained.

Index Terms: Ag(In, Ga)Se_2, three-stage, Ag diffusion, growth mechanism.

1. Introduction

Cu, (InGa)Se_2 (CIGS) is one of the most promising materials for photovoltaic applications and holds the world record conversion efficiency of 22.6% [1]. However, further increasing its conversion efficiency is both costly and difficult. Tandem solar cells are one recognized approach for overcoming this issue. Ag(In_xGa_{1-x})Se_2 ($0 \leq x \leq 1$) (AIGS) crystals are a promising candidate for the top cell of CIGS–based tandem solar cells owing to its identical crystal structure to CIGS, suitable optical properties. Additionally, it has a variable bandgap of 1.24 ($AgInSe_2$) [2] to 1.78 eV ($AgGaSe_2$) [3], achieved by tuning the Ga/(In+Ga) (Ga/III) atomic ratio, which satisfies the requirement of a wide bandgap material for the top cell [4]. There have been several reports on the application of AIGS thin films to solar cells [5]–[7], and a highest efficiency of 10.7% was achieved in our previous research [8]. As reported in our previous studies, growth processes play a very important role in

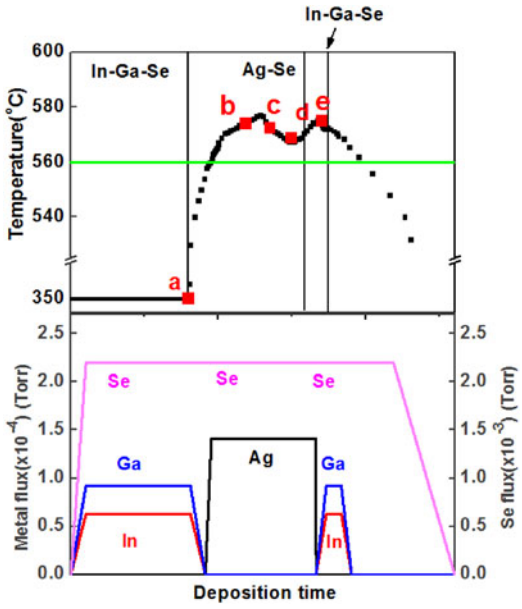

Fig. 1. Substrate temperature and metal flux profiles as a function of deposition time. Points a–e denote samples taken out of the chamber.

the performance of AIGS solar cells [9]. In the case of CIGS solar cells, the growth mechanism of CIGS films with both Cu-rich and Cu-poor compositions has already been reported [10], and can be described as: (In, Ga)$_2$Se$_3$ → Cu(In, Ga)$_5$Se$_8$ → Cu(In, Ga)$_3$Se$_5$ → Cu(In, Ga)Se$_2$. However, the growth mechanism of AIGS films by similar methods is still unknown. In this work, we report on a study designed to clarify the growth process of AIGS films by a three-stage method and propose a growth mechanism was based on the obtained results.

2. Experimental Method

AIGS films were fabricated on a Mo-coated soda lime glass substrate by a three-stage molecular beam epitaxy (MBE) method. Fig. 1 shows the substrate temperature and metal flux profiles as a function of deposition time during the deposition process. During the first stage, In, Ga, and Se with a pressure of 6×10^{-5}, 9×10^{-5}, and 2.3×10^{-3} Torr, respectively, were deposited on the substrate for 40 min at a substrate temperature of 350 °C. The substrate temperature was then increased to 570 °C. During the heating, the Ag flux (pressure of 1.3×10^{-4} Torr), which lasted for 40 min, was turned on when the substrate temperature reached 500 °C, which is marked as the starting point of the second stage. The temperature valley observable in Fig. 1 was caused by the accumulation of Ag-Se at the surface of the AIGS films, which is supposed to have larger heat emission coefficient than (In, Ga)$_2$Se$_3$ and AIGS, causing a decrease in the temperature of the substrate. During the third stage, In and Ga were deposited again to obtain the desired stoichiometric composition. The Se flux was kept constant throughout the deposition process to prevent the evaporation of In from the film. The details of the experimental method have been described in our previous study [9]. To investigate the growth mechanism of the AIGS films, samples were removed from the deposition apparatus at the points donated a–e in the figure for characterization. Sample a was removed at the end of the first stage, and was expected to have a γ phase In$_2$Se$_3$ structure, while samples b–d were removed during the second stage based on the Ag deposition time. Sample b was expected to have the intermediate phase of the growth process. Sample c was expected to show significant Ag accumulation near its surface. Sample d was taken at the end point of the second stage, and was expected to show a silver-rich composition. Sample e was removed at the end of the third stage, the

TABLE 1
Atomic Composition of Different Samples by EDS

Sample	Ag	In	Ga	Se	Ag/III
	Composition (at. %)				
a	*	5.40	34.78	59.54	0
b	16.05	3.78	24.33	55.84	0.57
c	20.73	7.47	15.88	55.92	0.89
d	26.83	4.84	15.64	55.92	1.31
e	23.53	3.19	21.92	51.36	0.94
Ref.	22.49	2.10	23.55	51.86	0.88

same as normally deposited AIGS films. To make a reference, AIGS film was also deposited by the 1-stage co-evaporation method (refers to Ref. in the following part), that is, the elemental fluxes of Ag, In, Ga, and Se were maintained at a constant value through out the deposition period. The total depositing time is the same as three-stage method (about 90 min) with a deposition temperature of 570 °C and the flux value was adjusted to make sure the same amount of elements was deposited. The aforesaid experiment was repeated three times to ensure reproducibility, and similar results were obtained.

A JEOL JSM-5510-5510LV scanning electron microscope (SEM) equipped with energy dispersive spectroscopy (EDS) was used to characterize the samples. SEM images were taken at an accelerating voltage of 10 kV, while EDS was conducted at an accelerating voltage of 20 kV. A Rigaku Hyper-RINT X-ray diffractometer (XRD) was used to characterize the phases of the as-fabricated AIGS films. The reactions occurring during the fabrication of the AIGS films by the three-stage method were proposed based on the obtained results.

3. Results and Discussion

3.1 Composition and Morphology of AIGS Films

Table 1 shows the atomic composition of the samples measured by EDS. Sample a had a composition of $(In, Ga)_2Se_3$ as expected, while samples b and c had a silver-poor composition. Sample d had an Ag/III ratio of 1.31, meaning that the film was Ag-rich as expected. Sample e had an Ag/III ratio of 0.94, suggesting that the AIGS film became silver-poor again during the third stage. In addition, the sample Ref. shows a Ag/III raio of 0.88, which is a favorable atomic ratio for AIGS solar cell. However, the In atomic ratio of sample Ref. is significantly lower than other samples due to the In evaporation because of high deposition temperature and no protection from Ag-Se layer. To account for any errors, the EDS measurements were carried out three times, and the data in the table is the average value of several points. Thus, any deviation of composition in the table should be experimentally significant. Fig. 2 shows the Ag/III atomic ratios of samples a–e plotted against deposition time. The plot is divided into silver-rich and silver-poor regions. Samples a, b and c fall in Ag-poor region with a Ag atomic ratio of 0, 0.57, and 0.89, respectively. The only the sample d that is taken out at the end of the second stage showed a silver-rich composition with a Ag atomic ratio of 1.31. After finishing the whole deposition process, the film shows a Ag poor composition (sample e) of 0.94.

Fig. 3 shows the surface morphology of samples a–e and Ref.. Sample a exhibited a very small grain size and flat surface, which is a typical morphology for $(In, Ga)_2Se_3$ films [11], while sample

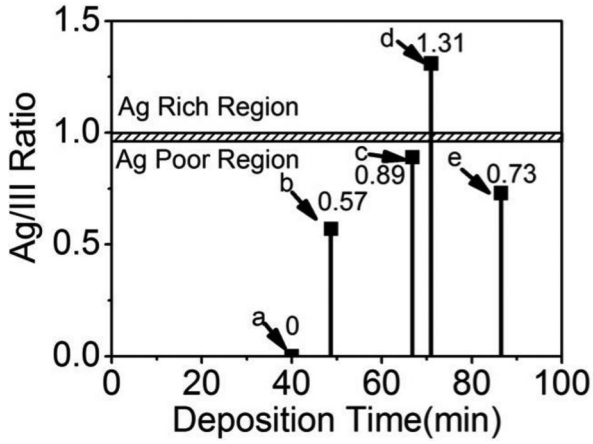

Fig. 2. Dependence of Ag/III atomic ratio of AIGS films on deposition time.

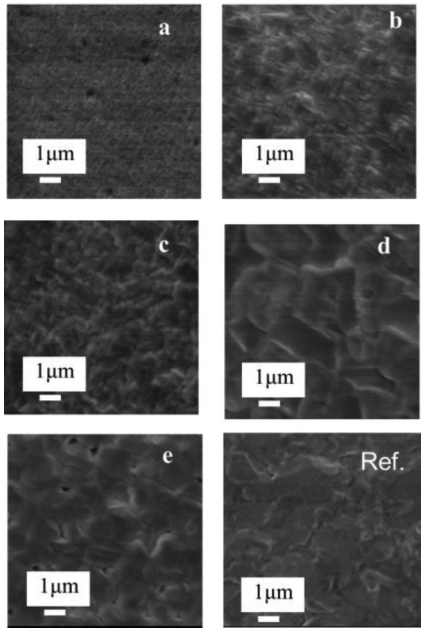

Fig. 3. Surface morphology of samples a–e and reference sample.

b contained some large grains surrounded by small (In, $Ga)_2Se_3$ grains. The large grains are over 1 μm, while the small grains are just several-ten nm. From sample b to d, the grain size increased obviously and grain boundaries became clearer. The grain size increases to around 2 μm for sample d. Sample e exhibited the morphology of a typical AIGS film, and its grain size was larger than 2 μm. in addition, the grain size of the sample Ref. is very irregular, where the large grain size is over 3 μm and small one is less than 1 μm, indicating the three-stage method promotes the film quality comparing with 1-stage method.

3.2 Diffusion Process of Ag Into (In, $Ga)_2Se_3$ Film

Fig. 4 shows the cross-sectional SEM images and distribution of silver measured by EDS of samples a–e. The color bar at the bottom of each EDS image indicates the strength of the silver signal from

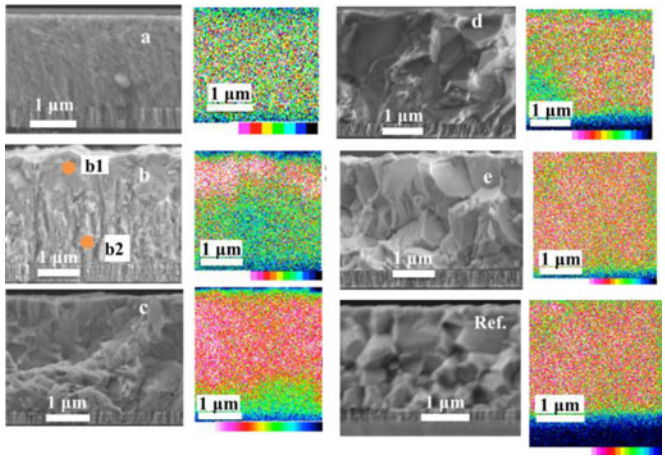

Fig. 4. Diffusion of Ag into (In, $Ga)_2Se_3$ films during the experiment. Samples marked a-e and Ref. reveal cross-sectional SEM image, while the correspondent right figure illustrate silver distribution in the AIGS film. SEM and EDS measurements were carried out at the same position. The color bar at the bottom of each EDS image indicates the strength of the Ag signal in the sample, increasing from right to left.

TABLE 2
Composition of AIGS Films at Point b1 and b2

Element	Ag (%)	In (%)	Ga (%)	Se (%)	Ga/III	Ag/III
b1	52.80	1.20	6.50	39.5	0.84	6.86
b2	1.50	4.60	33.3	60.6	0.88	0.04

the sample, increasing from right to left. Because sample a was an (In, $Ga)_2Se_3$ film, no EDS signal of silver was observed. Sample b showed a bilayer structure: the lower layer had the same morphology as the (In, $Ga)_2Se_3$ film of sample a and no Ag signal was observed, while the upper layer exhibited a very strong Ag signal, indicating a high Ag atom density. This result reveals that unlike copper in the case of CIGS, which diffuses very fast owing to its high diffusion coefficient and results in no copper accumulation in the film [9], significant silver accumulation occurred in the AIGS film owing to its slow diffusion caused by its low diffusion coefficient [12]. Table 2 shows the composition of b1 and b2 points (orange points) in Fig. 4(b) determined by point EDS measurement. Point b1 exhibited an extremely high Ag/III ratio, indicating severe Ag accumulation, while point b2 exhibited a very low Ag/III ratio and a Se/III atomic ratio of approximately 1.60, almost the same as (In, $Ga)_2Se_3$ film. This difference in composition between the two layers revealed that the upper layer was silver-rich and lower layer was silver-poor, indicating that the silver did not diffuse throughout the whole film. On the other hand, Ag distributes uniformly in the sample Ref. because Ag supply was constant during the deposition process and Ag will not accumulate in the film.

Sample c exhibited a larger grain size, and the (In, $Ga)_2Se_3$ part shrank to a very thin layer, as shown in the SEM image. Judging from the EDS image, the distribution of silver in this sample was still non-uniform, but was enhanced compared with that of sample b, and the silver-poor layer only existed near the Mo back contact. Sample d was that taken at the end of the second stage. The grain size continued to grow and silver diffused to the bottom of the film in this sample, but a silver-poor area could still be observed. For sample e, no significant silver accumulation could be observed

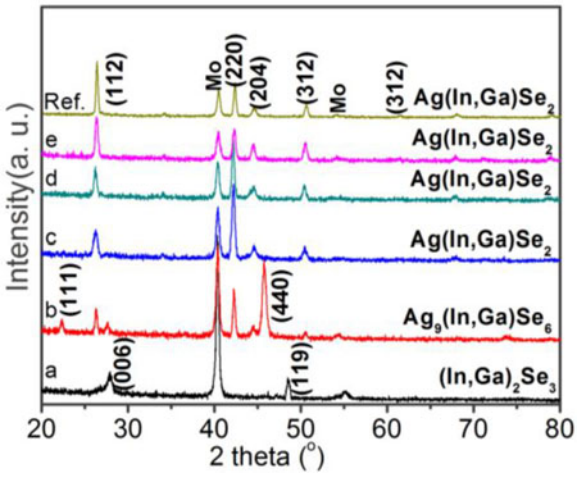

Fig. 5. XRD patterns of samples a-e and Ref.

except at certain points, indicating a much more uniform distribution of silver in the film. According EDS mapping of Ag in sample Ref, no accumulation of Ag was detected, showing a uniform Ag distribution. To reveal the phase transformations occurring during the deposition processes, the samples were next characterized by XRD.

3.3 Phase Transformation During the Deposition Process

Fig. 5 show the XRD patterns of samples a–e and Ref. The figure illustrates the phase change in the AIGS films during the different stages of the deposition process. The XRD pattern of the (In, Ga)$_2$Se$_3$ sample (a) could be indexed to the peaks of γ-In$_2$Se$_3$, indicating that sample a had a γ-In$_2$Se$_3$ phase with the defect wurtzite structure [13]. Peaks of γ-In$_2$Se$_3$ could also be observed in the XRD pattern of sample b, but their intensity was much weaker, and the (111) and (440) peaks of Ag$_9$GaSe$_6$ [14] were also observed. Besides, the (112), (220), and (204) peaks of AIGS were also present, meaning the sample contained a mixture of (In, Ga)$_2$Se$_3$, Ag$_9$GaSe$_6$, and AIGS phases. Although it seems that the formation of Ag$_9$(In, Ga)Se$_6$ was difficult at the beginning because of the low silver atomic ratio, the fact is that silver diffused into the (In, Ga)$_2$Se$_3$ layer very slowly, resulting in a silver-rich condition on the surface that made the formation of Ag$_9$GaSe$_6$ possible at the top layer of the sample. Thus, this result is in accordance with the silver distribution shown in the EDS results. For samples c–e and Ref., all the peaks could be well indexed to the structure of chalcopyrite AIGS films, and the peaks of (In, Ga)$_2$Se$_3$ disappeared, indicating that typical AIGS films had been deposited. The peak intensity of the (112) and (220) peaks, especially the (112) peak, was obviously increased. The (112)/(220) relative peak intensity increased from sample c to e, indicating that the preferred orientation of the film changed from (220) to (112).

Judging from the Ag$_2$Se-Ga$_2$Se$_3$ phase diagram of AgGaSe$_2$ film [15], films having silver-poor composition are mainly composed of a mixture of AgGaSe$_2$ and δ phases. At the beginning of the second stage, silver was deposited on the (In, Ga)$_2$Se$_3$ layer. Although the resulting film had a silver-poor composition, a silver-rich layer formed at the surface owing to the low diffusion coefficient of silver. This finding is also confirmed by the distribution of silver in sample b revealed by EDS; a silver-rich composition at the top as well as a (In, Ga)$_2$Se$_3$ layer at the bottom of the film were observed. As a result, the XRD pattern of the film showed a mixture of peaks of (In, Ga)$_2$Se$_3$, Ag$_9$GaSe$_6$, and AIGS. With the diffusion of silver, the sharply defined silver-rich and (In, Ga)$_2$Se$_3$ layers gradually disappeared, resulting in the domination of AIGS peaks in the XRD patterns of samples c, d, and e. Based on these results, it can be concluded that at the beginning of the second stage, silver became segregated on the surface of the film and formed a silver-rich intermediate

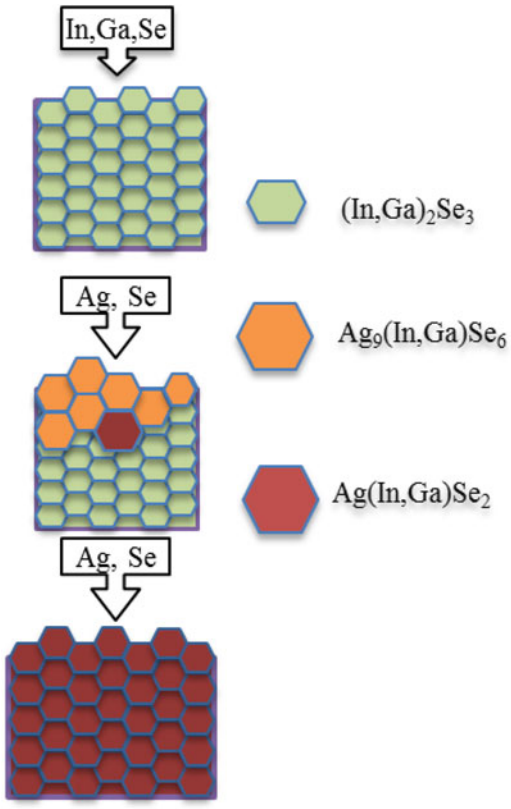

Fig. 6. Diagrams of crystal growth and phase changes in the AIGS films during the second stage.

phase, $Ag_9(In, Ga)Se_6$. With the increasing deposition of silver, the diffusion of silver was enhanced and formation of AIGS was also improved.

Diagrams of the phase changes occurring in the AIGS films during the three-stage deposition process is shown in Fig. 6. During the first stage, In, Ga, and Se formed $(In, Ga)_2Se_3$, as shown in reaction (1):

$$In + Ga + Se \rightarrow (In,\ Ga)_2Se_3 \tag{1}$$

$$(In,\ Ga)_2Se_3 + Ag + Se \rightarrow Ag_9\,(In,\ Ga)\,Se_6 + (In,\ Ga)_2Se_3 + Ag(In,\ Ga)Se_2. \tag{2}$$

At the beginning of the second stage, a small amount of silver was deposited on the $(In, Ga)_2Se_3$. The whole film showed a silver-poor composition, but silver segregated on the surface owing to its low diffusion coefficient. As a result, the silver-rich phase $Ag_9(In, Ga)Se_6$ was formed at the surface, leaving the rest of the film a mixture of $Ag(In, Ga)Se_2$ and $(In, Ga)_2Se_3$. This process is described in reaction (2):

$$Ag_9\,(In,\ Ga)\,Se_6 + (In,\ Ga)_2Se_3 + Ag \rightarrow Ag(In,\ Ga)Se_2\,(\text{silver rich}) \tag{3}$$

$$Ag(In,\ Ga)Se_2 + (In,\ Ga)_2Se_3 \rightarrow Ag(In,\ Ga)Se_2\,(\text{silver poor}) \tag{4}$$

With the further deposition of silver, its diffusion was enhanced, and silver-rich AIGS film was obtained at the end of the second stage. In the final stage, the film was converted to typically deposited silver-poor AIGS film. This process is shown in reactions (3) and (4).

Thus, we have illustrated the growth mechanism of AIGS film fabricated by a three-stage Co-evaporation MBE method. Note that the present analysis is only applicable to AIGS films fabricated

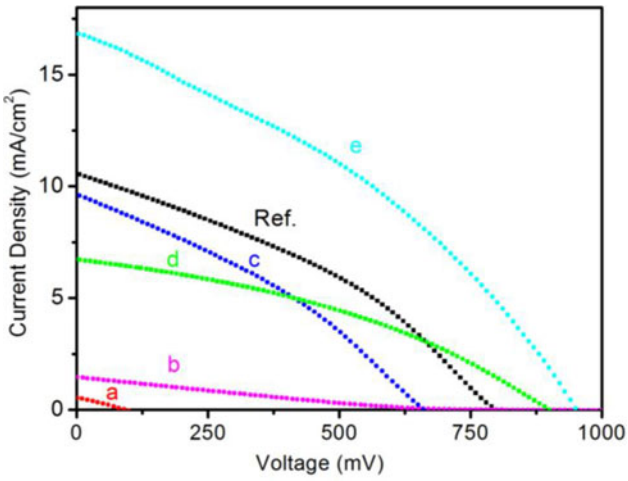

Fig. 7. I-V curves of solar cells with samples a-e as the absorber layer.

TABLE 3
Performance of Solar Cells With Samples a-e as the Absorber Layer

Sample	V_{oc} (mV)	J_{sc} (mA/cm^2)	FF	E_{ff} (%)
a	92.4	0.5	23.0	0.0
b	746.9	1.5	20.5	0.2
c	901.2	6.7	36.9	2.2
d	660.1	9.6	32.7	2.1
e	930.4	16.8	45.4	7.1
Ref.	797.7	10.7	35.1	3.0

by this method and is based on the fact that silver has a low diffusion coefficient. The growth mechanism of AIGS films deposited by other methods such as one-stage evaporation [16] or hot press method [17] will be different. Also, the diffusion of silver is significantly influenced by the temperature of the substrate. At a high substrate temperature, the diffusion of silver is enhanced. Thus, the accumulation of silver will be lower and the formation of a silver-rich phase at the surface will be difficult. However, a high temperature is not suitable during the deposition process because of In evaporation, as reported in our previous study [8].

3.4 Performance of the Solar Cell

Samples a-e and Ref. were used to fabricate solar cells. The I-V curves of the obtained solar cells are shown in Fig. 7, and the output parameters of the devices are summarized in Table 3. Almost no solar cell property is detected for sample a because $(In, Ga)_2Se_3$ and CdS can hardly form a pn junction. Sample b shows a sever Ag poor composition; leading to 0.2% efficiency and low FF as well. For samples c and d, AIGS phase gradually forms, resulting in improved efficiency of about 2%. The possible reason that sample c shows higher Voc than d is that Ag rich composition in sample d leads to larger leak current and stronger recombination in the film, which results in lower Voc. The performance of the solar cells increases significantly after the three-stage process finishing and an efficiency of 7.1% with a high V_{oc} of 930.4 mV was obtained for sample e, which was deposited as a normal AIGS film. Although the sample Ref. shows stoichiometric composition,

the conversion efficiency is just 3%, with low FF due to the disrupted Ga grade in the film, indicating that three-stage is effective in improving solar cell performance.

4. Conclusion

The growth process of AIGS films fabricated by a three-stage MBE method was studied. Silver accumulates easily on the surface of the film because of the low diffusion coefficient of Ag. This accumulation leads to the formation of an intermediate phase, Ag_9(In, Ga)Se_6, at the preliminary stage of the deposition process, although the whole film shows a silver-poor composition. With increasing deposition of silver, its diffusion is enhanced, and the silver distribution of the film becomes more homogeneous. After the second stage, the film has a silver-rich composition, and is converted to silver-poor after the third stage, which is necessary for high efficiency AIGS solar cells. An AIGS film growth model was suggested as follows: (In, Ga)$_2Se_3$ $\rightarrow$ Ag_9 (In, Ga)Se_6 at the surface and (In, Ga)$_2Se_3$ at the bottom of the film $\rightarrow$ AIGS film. A high V*oc* of about 930 mV was obtained for a normal AIGS solar cell with an efficiency of 7.1%. Although the 1-stage deposited reference sample shows stoichiometric composition and uniform Ag distribution, solar cell performance is low, indicating the three-stage method is an effective approach for fabricating high-efficiency AIGS solar cells.

Acknowledgment

This work was performed while X. F. Zhang was a postdoc at Tokyo Tech, Meguro-Ku, Tokyo, 152-8550, Japan.

References

[1] P. Jackson, R. Wuerz, D. Hariskos, E. Lotter, W. Witte, and M. Powalla, "Effects of heavy alkali elements in Cu(In, Ga)Se2 solar cells with efficiencies up to 22.6%," *Phys. Status Solidi RRL*, vol. 10, no. 8, pp. 583–586, 2016.
[2] H. Mustafa, D. Hunter, A. K. Pradhan, U. N. Roy, Y. Cui, and A. Burger, "Synthesis and characterization of $AgInSe_2$ for application in thin film solar cells," *Thin Solid Films*, vol. 515, pp. 7001–7004, 2007.
[3] H. Matsuo, K. Yoshino, and T. Ikari, "Dependence of Ag/Ga composition ratio in $AgGaSe_2$ thin film," *Phys. Status Solidi C*, vol. 3, pp. 2639–2643, 2006.
[4] S. P. Bremner, M. Y. Levy, and C. B. Honsberg, "Analysis of tandem solar cell efficiencies under AM1.5G spectrum using a rapid flux calculation method," *Prog. Photovolt.: Res. Appl.*, vol. 16, pp. 225–233, 2008.
[5] T. Nakada *et al.*, "Chalcopyrite thin-film tandem solar cells with 1.5 V open-circuit-voltage," in *Proc. IEEE 4th World Conf. Photovolt. Energy Convers.*, 2006, pp. 400–403.
[6] K. Yamada, N. Hoshino, and T. Nakada, "Crystallographic and electrical properties of wide gap Ag(In_{1-x},Ga_x)Se_2 thin films and solar cells," *Sci. Technol. Adv. Mater.*, vol. 7, pp. 42–45, 2006.
[7] T. Nakada, K. Yamada, R. Arai, H. Ishizaki, and N. Yamada, "Novel wide-band-gap Ag($In_{1-x}Ga_x$)Se_2 thin film solar cells," in *Proc. Mater. Res. Soc.*, vol. 865, 2005, pp. F11.1–F11.6.
[8] X. F. Zhang, T. Kobayashi, Y. Kurokawa, S. Miyajima, and A. Yamada, "Deposition of Ag(In, Ga)Se_2 solar cells by a modified three-stage method using a low-temperature-deposited Ag–Se cap layer," *Jpn. J. Appl. Phys.*, vol. 52, pp. 055801-1–055801-5, 2013.
[9] X. F. Zhang, T. Kobayashi, Y. Kurokawa, and A. Yamada, "Growth of Ag(In, Ga)Se_2 films by modified three-stage method and influence of annealing on performance of solar cells," *Jpn. J. Appl. Phys.*, vol. 51, pp. 10NC05-1–10NC05-4, 2012.
[10] S. Nishiwaki, T. Sato, S. Hayashi, Y. Hashimoto, T. Negami, and T. Wada, "Physical vapor deposition of Cu(In, Ga)Se_2 films for industrial application," *J. Mater. Res.*, vol. 14, pp. 4514–4520, 1999.
[11] T. Mise and T. Nakada, "Microstructural properties of (In, Ga)$_2Se_3$ precursor layers for efficient CIGS thin-film solar cells," *Sol. Energy Mater. Sol. Cells*, vol. 93, pp. 1000–1003, 2009.
[12] B. F. Dyson, T. Anthony, and D. Turnbull, "Interstitial diffusion of copper and silver in lead," *J. Appl. Phys.*, vol. 37, pp. 2370–2374, 1966.
[13] M. Emziane and R. L. Ny, "Crystallization of In_2Se_3 semiconductor thin films by post-deposition heat treatment. Thickness and substrate effects, thickness and substrate effects," *J. Phys. D: Appl. Phys.*, vol. 32, pp. 1319–1328, 1999.
[14] N. H. Kim and R. S. Feigelson, "Surface migration and volume diffusion in the $AgGaSe_2-Ag_2Se$ system," *J. Mater. Res.*, vol. 7, pp. 1215–1220, 1992.
[15] J. C. Mikkelsen, "Ag_2Se–Ga_2Se_3 pseudobinary phase diagram," *Mater. Res. Bull.*, vol. 12, pp. 497–502, 1977.
[16] H. Matsuo, K. Yoshino, and T. Ikari, "Dependence of Ag/Ga composition ratio in $AgGaSe_2$ thin film," *Phys. Status Solidi*, vol. 3, no. 8, pp. 2639–2643, 2006.
[17] A. Kinoshita, H. Matsuo, K. Yoshino, T. Ikari, and K. Kakimoto, "Growth of $AgGaSe_2$ crystals by hot-press method," *Phys. Status Solidi*, vol. 3, no. 8, pp. 2903–2906, 2006.